Subchronic Oral Exposure to Benzo(a)pyrene Leads to Distinct Transcriptomic Changes in the Lungs That Are Related to Carcinogenesis

Sarah Labib,* Carole Yauk,* Andrew Williams,* Volker M. Arlt,† David H. Phillips,† Paul A. White,* and Sabina Halappanavar*,1

*Environmental and Radiation Health Sciences Directorate, Health Canada, Ottawa, Ontario K1A 0K9, Canada; and †Analytical and Environmental Sciences Division, King's College London, London, SE1 9NH, U.K.

[1]To whom correspondence should be addressed at Tunney's Pasture Bldg. 8 (P/L 0803A), 50 Columbine Driveway, Ottawa, Ontario K1A 0K9, Canada. Fax: (613) 941-8530. E-mail: sabina.halappanavar@hc-sc.gc.ca.

We have previously shown that acute oral exposure to the environmental carcinogen benzo(a)pyrene (BaP) elicits comparable levels of DNA adducts, but distinct transcriptomic changes, in mouse lungs and livers, the two main BaP bioactivating organs. Oral BaP exposure is predominantly associated with lung cancer and not hepatic cancer in some animal models, suggesting that gene expression differences may provide insight into the drivers of tissue-specific carcinogenesis. In the present study, we examine pulmonary DNA adduct formation, *lac*Z mutant frequency, and mRNA profiles in adult male MutaMouse following subchronic (28 day) oral exposure to BaP (0, 25, 50, and 75 mg/kg/day) and sacrificed 3 days postexposure. The results are compared with those obtained from livers of the same mice (previously published). Although there was a 1.8- to 3.3-fold increase in the levels of DNA adducts in lung compared with liver, the *lac*Z transgene mutant frequency was similar in both tissues. At the transcriptomic level, a transition from activation of the DNA damage response p53 pathway at the low dose to the induction of genes involved in angiogenesis, evasion of apoptosis and growth signals at the high doses was evident only in the lungs. These results suggest that tissue DNA adducts and mutant frequency are sensitive markers of target tissue exposure and mode of action, whereas early changes in gene expression may provide a better indication of the likelihood of carcinogenic transformation in selected tissues. Moreover, the study provides new information on the underlying mechanisms that contribute to tissue-specific responses to BaP.

Key Words: Gene expression; p53 response; lung cancer; genotoxicity; DNA adducts; Mutant frequency.

Benzo(a)pyrene (BaP) is a well-studied polycyclic aromatic hydrocarbon (PAH) that is found in cigarette smoke, indoor and outdoor air, and charred meats. Metabolic activation of BaP by cytochrome P450 (CYP) enzymes, namely CYP1a1 and CYP1b1, results in the generation of several BaP metabolites, including BaP-7,8-diol-9,10-epoxide (BPDE), a highly reactive form of BaP. BPDE is the primary metabolite of BaP that covalently binds DNA and forms DNA adducts (Baird *et al.*, 2005). These DNA adducts, if left unrepaired, can cause mutations in genes involved in xenobiotic metabolism, tumor suppression, or oncogenes leading to tumor development. The International Agency for Research on Cancer (IARC) has recently upgraded their classification of BaP to a Group 1 (i.e., known human) carcinogen (Baan *et al.*, 2009). Exposure to BaP leads to tumor formation in animal models, and epidemiologically, a link between BaP exposure and cancer incidence in humans has been established (OEHHA, 2010). In addition to being carcinogenic and mutagenic, BaP is a known immunosuppressant (Dean *et al.*, 1983). It can also alter cell cycle progression (Solhaug *et al.*, 2005), induce inflammation (Qamar *et al.*, 2012), and impair DNA repair and apoptotic processes (Solhaug *et al.*, 2005) leading to aberrant cellular functioning.

The primary site of BaP metabolism is the liver; however, hepatocarcinogenesis is rare in humans and inconsistent in animals (OEHHA, 2010). Lung carcinogenesis, on the other hand, is prevalent in mice exposed orally to BaP (Stoner *et al.*, 1984; Wattenberg and Leong, 1970), including MutaMouse (Hakura *et al.*, 1998). This is explained by greater BaP retention in the lung (Galván *et al.*, 2005; Harrigan *et al.*, 2004), higher induction of CYP1a1 and CYP1b1 in the lung tissue (Harrigan *et al.*, 2006), and higher levels of BPDE-DNA adducts in the lungs compared with the liver (Harrigan *et al.*, 2004). Indeed, the levels of BaP-induced DNA adducts in any tissue at a given time is a function of metabolic conversion of BaP to its DNA-reactive metabolites via phase I xenobiotic metabolism, phase II detoxification, the rate of adduct repair, and the cell turnover rate, collectively suggesting that tissue dynamics and BaP response between lung and liver tissues likely differ.

Our previous work examined global gene expression changes in the lungs of adult male mice following acute exposure to 150 and 300 mg/kg BaP by oral gavage for three consecutive days

and sacrificed 4h postexposure (Halappanavar *et al.*, 2011). The pulmonary transcriptomic response included changes in biological pathways involved in B-cell receptor (BCR) signaling, inflammation, and DNA damage response. We also noted that the response in the lung tissue was different, and in some respects, much more pronounced than livers from the same mice. Oxidative stress, xenobiotic metabolism, aryl hydrocarbon receptor (AhR) signaling, and glutathione metabolism were among the common pathways that were affected in both tissues, whereas negative regulation of the BCR signaling, indicative of potential primary immunodeficiency, was unique to the lung tissue. However, both tissues exhibited similar levels of DNA adducts, suggesting that evidence of higher levels of tissue DNA adducts are not sufficient to predict the observed transcriptomic differences in lungs and livers. Although the study was conducted at very high doses of BaP, the findings support the hypothesis that tissue-specific mechanisms are at work and that differential regulation of the known biological pathways associated with cancer formation could explain the selective targeting of lungs for carcinogenesis.

In the present study, we explore further the potential of early BaP-induced gene expression changes to identify the tissue-specific events that may eventually lead to carcinogenic transformation following BaP exposure. We globally profile the pulmonary transcriptome and measure in parallel the induced frequency of mutations and DNA adducts (known predictors of genotoxicity-mediated cancer) in the lung tissues of adult male mice repeatedly exposed to 25, 50, and 75 mg/kg BaP for 28 consecutive days by oral gavage and sacrificed 3 days postexposure. The results are compared and interpreted in light of the differential biological responses reported for the lungs and livers of mice following both acute (Halappanavar *et al.*, 2011; Yauk *et al.*, 2011) and subchronic (Malik *et al.*, 2012) exposures to BaP.

MATERIALS AND METHODS

Animal treatment. Adult (25 weeks old) male mice of MutaMouse strain (transgenic mouse strain 40.6) were exposed to BaP (Sigma Aldrich, Canada) as described previously (Malik *et al.*, 2012). In brief, animals were dosed daily via oral gavage for 28 days with varying doses of BaP (0, 25, 50, and 75 mg/kg body weight/day) dissolved in olive oil. Each dose group contained five animals. Mice were sacrificed by cardiac puncture under isoflorane anesthesia 72h following the final exposure. The right lobe of the lung was excised, flash frozen in liquid nitrogen, and stored at −80°C until use. For the duration of the experiment, food (2014 Teklad Global standard rodent diet) and water were provided *ad libitum*, and mice were caged individually in plastic film isolators (Harlan Isotec, U.K.) on a 12-h light/12-h dark cycle. Mice were bred, maintained, and treated in accordance with the Canadian Council for Animal Care Guidelines and approved by Health Canada's Animal Care Committee.

Tissue selection. The major exposures to BaP occur via the oral route (drinking and feed) (Hettemer-Frey and Travis, 1991). The organs directly affected by BaP as a consequence of oral exposure include stomach, esophagus, tongue, and larynx (Culp *et al.*, 1998). However, studies conducted by Stoner *et al.* (1984) and Wattenberg and Leong (1970) showed lung and liver to be equally impacted by BaP (oral gavage) and, moreover, revealed sensitivity of lung for tumor development in comparison with liver. In alignment with these reports, our previous work (Halappanavar *et al.*, 2011; Yauk *et al.*, 2011) revealed lung-specific regulation of the biological processes known to be associated with cancer formation. Thus, in the present study, we have investigated transcriptional responses in lung and liver. The results of the study may also help address the importance of considering the multiorgan toxicity in calculating the risk associated with chemicals, such as BaP.

Tissue DNA extraction. The frozen lung and liver tissues were sliced randomly. Genomic DNA was isolated from a random tissue section for measuring the levels of DNA adducts and transgene mutant frequency. In brief, lung tissue was minced and degassed to remove all traces of air in the alveoli. Livers were homogenized in ice cold TMST buffer (50mM Tris, pH 7.6, 3mM magnesium acetate, 250mM sucrose, 0.2% Triton X-100) as described in the study by Douglas *et al.* (1994). The minced tissue was washed twice in cold PBS and lysed in 10mM Tris, pH 7.6, 10μM EDTA, 100μM NaCl, and 1% SDS overnight at 37°C on a rotating platform. The lysate was digested with proteinase K (1 mg/ml lysis buffer). DNA was isolated using a serial phenol/chloroform/isoamyl alcohol (25:24:1) and chloroform/isoamyl alcohol (24:1) extraction (Renault *et al.*, 1997). DNA was precipitated in ethanol and dissolved in Tris-EDTA buffer (10mM Tris, pH 7.6, 500mM EDTA). DNA was stored at 4°C until use.

DNA adduct analysis. DNA adduct formation in each sample was determined using the nuclease P1 digestion enrichment version of the ^{32}P-postlabeling assay as described previously (Phillips and Arlt, 2007) with minor modifications. Briefly, 4 μg of DNA was digested overnight with micrococcal nuclease (288 mUnits, Sigma, cat. no. N3755) and calf spleen phosphodiesterase (1.2 mUnits, MP Biomedicals, cat. no. 100977), enriched, and labeled as described elsewhere (Phillips and Arlt, 2007). Radiolabeled adducted nucleotide biphosphates were separated by thin-layer chromatography on polyethyleneimine-cellulose plates (Macherey-Nagel, Düren, Germany) with the following chromatographic conditions (Arlt *et al.*, 2008): D1, 1.0M sodium phosphate, pH 6; D3, 4.0M lithium formate, 7.0M urea, pH 3.5; D4, 0.8M LiCl, 0.5M Tris, 8.5M urea, pH 8. Chromatographs were scanned using a Packard Instant Imager (Canberra Packard, Downers Grove USA), and DNA adduct levels (relative adduct labeling) were calculated from the adduct counts per minute (cpm), the specific activity of [γ-^{32}P]ATP, and the amount of DNA (pmol of DNA-P) used. An external BPDE-DNA standard was used for identification of BaP-DNA adducts. Results are expressed as DNA adducts/10^8 nucleotides.

LacZ mutant frequency (positive selection). The transgene *lacZ* mutant frequency in lungs was determined using the P-gal (phenyl-β-D-galactopyranoside) positive selection assay as described in the study by Vijg and Douglas (1996) and Lambert *et al.* (2005). The λgt10*lacZ* DNA was rescued from the genomic DNA using the Transpack lambda packaging system (Stratagene). The packaged phage particles were mixed with host bacterium (*Escherichia coli lacZ⁻*, *gal*E⁻, *rec*A⁻, pAA119 with *gal*T and *gal*K), plated on minimal medium containing 0.3% (w/v) P-Gal, and incubated overnight at 37°C. Total plaque-forming units (pfu) were measured on concurrent titers that did not contain P-Gal. Mutant frequency is expressed as the ratio of the number of mutant pfu to total pfu. Mutant frequency data analysis was performed as described previously (Malik *et al.*, 2012).

RNA extraction and purification. Total RNA was isolated for gene expression analysis and qRT-PCR validation as described previously (Halappanavar *et al.*, 2011). Briefly, total RNA was extracted from the lungs using TRIzol reagent (Invitrogen) and purified using RNeasy Mini Kit (Qiagen, Canada). The RNA quantity and purity were checked using a NanoDrop Spectrophotometer (ThermoFisher Scientific, Canada). The RNA integrity was determined using an Agilent 2100 Bioanalyzer (Agilent Technologies, Canada). The samples showing A_{260}/A_{280} ratios between 2.1 and 2.2 and having RNA integrity number above 7.5 were used for further analysis.

Microarray hybridization and analysis. Double-stranded cDNA and cyanine-labeled cRNA were synthesized (Agilent Linear Amplification Kits, Agilent Technologies) from 250 ng of total RNA from each sample and universal reference total RNA (Stratagene, Canada). Cyanine-labeled cRNA targets were *in vitro* transcribed using T7 RNA polymerase and purified by RNeasy Mini Kit (Qiagen). From each (sample and reference) labeled sample, 825 ng of cRNA was hybridized to Agilent 4×44K oligonucleotide microarrays (Agilent Technologies) at 60°C overnight (16 h) in the Agilent SureHyb hybridization chamber. Arrays were washed and scanned on an Agilent G2505B Scanner according to manufacturer's recommendations. Feature extraction software version 10.7.3.1 (Agilent Technologies) was used to extract the data.

A reference design (Kerr and Churchill, 2001) was used to analyze mRNA expression as described previously (Malik *et al.*, 2012). All analyses were conducted in the R (R-Development-Core-Team, 2010) environment using the MAANOVA library (Wu, 2010). The background fluorescence was measured using the negative control (−)3×SLv1 probes; probes with median signal intensities less than the trimmed mean (trim = 5%) plus three trimmed standard deviations of (−)3×SLv1 probe were flagged as absent (within the background signal). Probes were considered present if at least four of the five samples within a condition had signal intensities greater than three trimmed standard deviations above the trimmed mean of the (−)3×SLv1 probes (background signal). Data were normalized using the transform.madata() function using the glowess option with a span of 0.1. Ratio intensity plots and heat maps for the raw and normalized data were constructed to identify outliers. One sample (50 mg/kg group) was removed from the analysis based on clustering. The statistical model for this analysis included fixed effects of array and treatment condition and was applied to the $\log_2$ of the absolute intensities. Differentially expressed transcripts (upregulated or downregulated relative to olive oil–treated control mouse lung samples) were determined using the Fs statistic option in the matest() function. The *p* values for all statistical tests were estimated by the permutation method with residual shuffling, and false discovery rate (FDR) adjusted *p* values were estimated using the adjPval() function. The fold change calculations were estimated as described previously (Malik *et al.*, 2012). Significant genes were selected based on a FDR adjusted *p* value < 0.05 for any BaP exposed versus control contrast.

qRT-PCR array validation. Mouse pathway-specific PCR array (cancer-PAMM-033, SABiosciences) and custom PCR arrays consisting of 172 genes in total were employed to validate the microarray results. Genes for the custom array were selected based on their implication in biological processes relevant to lung carcinogenesis. These genes included statistically significant differentially expressed genes (FDR adjusted *p* < 0.05), differentially expressed genes that exhibited high fold changes (fold rank only) but were not statistically significant, and genes that were differentially regulated (FDR adjusted *p* < 0.05) in the livers from the same mice (Malik *et al.*, 2012). In brief, 0.8 µg of total lung tissue RNA (*n* = 5/group) from each sample was reverse transcribed using RT² First Strand Kit (SABiosciences). Real-time PCR was performed using RT² SYBR Green PCR Master Mix on a CFX96 real-time detection system (Bio-Rad, Canada). Threshold cycle values for each well were averaged. Relative gene expression was determined according to the comparative Ct method and normalized to reference RNAs *Hprt1*, *Gapdh*, and *Actb* housekeeping genes for the Cancer Pathway array and to reference RNAs *Gusb* and *Hprt1* housekeeping genes for the custom arrays. Transcripts were further normalized by subtracting the median delta Ct value for each sample. Differential expression was determined with a two-sample bootstrap test using R software (R-Development-Core-Team, 2010). The fold change was estimated using the ratio of the arithmetic mean of the treated sample to the mean of the control samples. Standard errors for the fold change values were estimated using the bootstrap test (Efron and Tibshirani, 1993).

Bioinformatics. All mRNA data are deposited in the NCBI Gene Expression Omnibus database under accession numbers GSE35718 (lung) and GSE24910 (liver). Following normalization, biological functions perturbed in response to BaP were identified using functional annotation clustering in the Database for Annotation, Visualization, and Integrated Discovery (DAVID)

(Huang da *et al.*, 2009) and the Kyoto Encyclopedia of Genes and Genomes (KEGG) (Kanehisa and Goto, 2000). The biological and molecular functions of genes that were significantly differentially expressed (FDR adjusted $p \leq 0.05$ or FDR adjusted $p \leq 0.1$ and fold change ≥ 1.5) following exposure to BaP treatment were analyzed and explored in Ingenuity Pathway Analysis (IPA, Ingenuity Systems, Redwood City, CA). Molecular relational networks of genes modulated by BaP in lung tissue enriched for cancer function were generated using IPA. Each molecule was overlaid onto a global molecular network developed from information contained in the Ingenuity Knowledge Base. Networks were generated based on their connectivity. All relationships are supported by at least one reference from the literature.

RESULTS

Daily exposure to 25, 50, and 75 mg/kg BaP for 28 consecutive days caused no overt signs of toxicity, and there was no significant body weight loss in any of the exposed mice compared with vehicle-treated controls.

BaP-Induced DNA Adduct Formation in Lung and Liver Tissue

The presence of DNA adducts indicates the development of premutagenic lesions following a chemical exposure. The ^{32}P-postlabeling technique was employed to measure BaP-induced DNA adducts in the lung tissues of mice exposed to 0, 25, 50, and 75 mg/kg BaP for 28 consecutive days (Fig. 1a). BaP-7,8-diol-9,10-epoxide-N^2-deoxyguanosine (dG-N^2-BPDE) was identified as the main adduct as reported previously (Lemieux *et al.*, 2011). No adducts were detected in mice dosed with vehicle control. DNA adduct formation by BaP was dose dependent. Although liver DNA adducts were analyzed in these samples previously (Lemieux *et al.*, 2011; Malik *et al.*, 2012), these data were not used. Instead, ^{32}P postlabeling was repeated in these samples in order to ensure that the protocols in both liver and lung were identical and performed in the same lab. Similar to results observed in the lungs, dG-N^2-BPDE was the main adduct identified in liver, and adduct levels increased in a dose-dependent manner (Fig. 1a). However, the frequency of DNA adducts in liver was significantly lower than in lung tissue for each dose (Bonferroni-corrected *p* value ≤ 0.05), suggesting that lung tissue is more susceptible to DNA damage caused by BaP.

Mutagenic Activity of BaP in the Lung Tissue

The MutaMouse contains around 29 +/− 4 (Shwed *et al.*, 2010) copies of λgt10*lac*Z shuttle vector stably integrated in the mouse genome, thus permitting *in vivo lac*Z mutant frequency analysis. In agreement with the DNA adduct results, a dose-dependent increase in mutant frequency was observed (Fig. 1b) in lung tissues. Compared with the vehicle controls, a 5.2-, 13-, and 18.6-fold increase was seen in the 25, 50, and 75 mg/kg dose groups, respectively. Mice gavaged with pure olive oil (vehicle) yielded a low spontaneous *lac*Z mutant frequency. No significant differences between the lung and liver tissues were observed for *lac*Z mutant frequency.
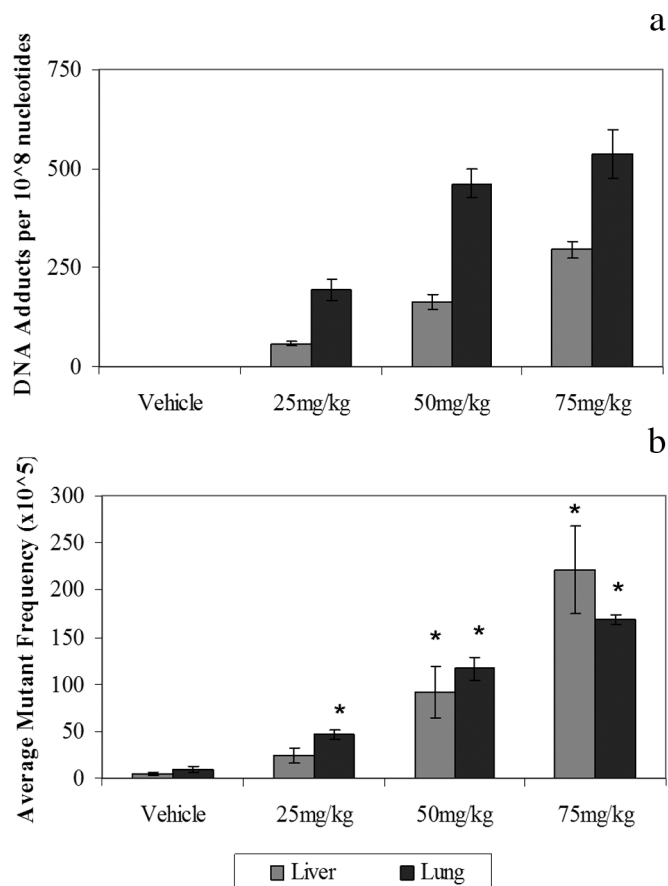
FIG. 1. DNA adduct formation (a) and *lac*Z mutant frequency (b) in the lungs and livers from MutaMouse subchronically exposed to BaP. Levels of dG-N^2-BPDE adducts were determined using the nuclease P1 enrichment version of the ^{32}P-postlabeling method. Data are represented as average ± SEM (*n* = 5 mice/group). ND, not detected. Average *lac*Z mutant frequency was determined using the P-Gal positive selection assay. Values shown are average frequencies ×10^5 ± SEM. Asterisk (*) indicates significance by Student's *t*-test (*p* < 0.01) compared with controls. Transgene mutant frequency data for the liver are from the study by Malik *et al.* (2012).

### General Overview of Pulmonary Gene Expression Profiles

Repeated oral gavage of mice with BaP induced significant changes in the expression of many genes in the lung tissue. Microarray Analysis of Variance (MAANOVA) analysis revealed 20, 145, and 373 unique probes that were differentially expressed (upregulated or downregulated) with a fold change ≥ 1.5 in either direction, and an FDR adjusted $p ≤ 0.05$ in the 25, 50, and 75 mg/kg exposure groups compared with controls, respectively (Supplementary File 1). The complete lung microarray data set is available through the Gene Expression Omnibus at NCBI (http://www.ncbi.nlm.nih.gov/geo/), accession number GSE35718. Hierarchical cluster analysis on all differentially expressed genes (FDR $p ≤ 0.05$, fold change ± 1.5) revealed that all treatment groups clustered separately from the control (Supplementary File 2); thus, a clear treatment effect was observed as a result of exposure to BaP.

Among the differentially expressed genes, 297 were upregulated and 90 were downregulated. Cyclin-dependent kinase inhibitor 1A (*Cdkn1a*), growth differentiation factor 15 (*Gdf15*), carboxylesterase 5 (*Ces5*), pleckstrin homology–like domain, family A, member 3 (*Phlda3*), multimerin 2 (*Mmrn2*), cyclin G1 (*Ccng1*), serum amyloid A 3 (*Saa3*), and sestrin 2 (*Sesn2*) were the most upregulated genes in all the dose groups. The most downregulated genes included Sarcolipin (*Sln*), myomesin 2 (*Myom2*), and tropomyosin 1, alpha (*Tpm1α*) in the 75 mg/kg group; chitinase 3-like 3 (*Chi3l2*) and gastrin releasing peptide (*Grp*) in the 50 mg/kg group; and sineoculis-related homeobox 1 homolog (*Six1*) (*Drosophila*) and ras homolog gene family member U (*Rhou*) in the 25 mg/kg dose group. Twenty-five probes representing 23 genes were commonly altered between the dose groups with an FDR $p ≤ 0.05$ in at least one dose group (Table 1). The observed transcriptomic response was dose dependent.

Gene ontology analysis was employed to assign biological processes and functional categories to significant genes (FDR $p ≤ 0.05$, fold change ≥ 1.5) in DAVID. Biological functions perturbed in response to BaP were identified using functional annotation clustering in DAVID (Supplementary file 3a). Significant functional enrichment (score > 2.0) was found for biological processes including extracellular signaling, cell adhesion, angiogenesis, apoptosis, and regulation of cell growth in all dose groups. Further combined analysis employing DAVID and KEGG pathways revealed that the altered genes are associated with specific biological pathways, including p53 signaling, molecular mechanisms of cancer, small cell lung cancer, extracellular membrane receptor interaction, and focal adhesion (Supplementary File 4a).

In addition to the analysis described above, we relaxed the FDR adjusted p value to include genes that exhibit FDR $p ≤ 0.1$ and fold change ≥ 1.5 to see whether we had missed any important genes in the pathways described above as a consequence of the stringent MAANOVA analysis. Using this criterion, 47, 181, and 429 genes in the 25, 50, and 75 mg/kg dose groups, respectively, were differentially altered. Fifty-one additional genes were identified by relaxing the p value cutoff (Supplementary file 6). DAVID analysis (Supplementary files 3b and 4b) as described above revealed three new functional categories: cell-to-cell and cell-to-matrix interactions, protein maturation, and inflammatory response. An in-depth functional analysis using IPA on these genes (FDR $p ≤ 0.1$ and fold change ≥ 1.5) revealed that the altered genes were associated with multiple functions, such as cancer, cell death, cell cycle, cellular growth and proliferation, cellular movement, DNA replication and repair, inflammatory response, and tumor morphology (Fig. 2a). Because the present work is focused on finding perturbations in pathways associated with carcinogenic transformation in the lung tissue, a subanalysis on specific genes that were grouped under the functional group "cancer" was performed. The subanalysis revealed that a majority of the genes from this group were mainly associated with the p53 signaling pathway

a

b
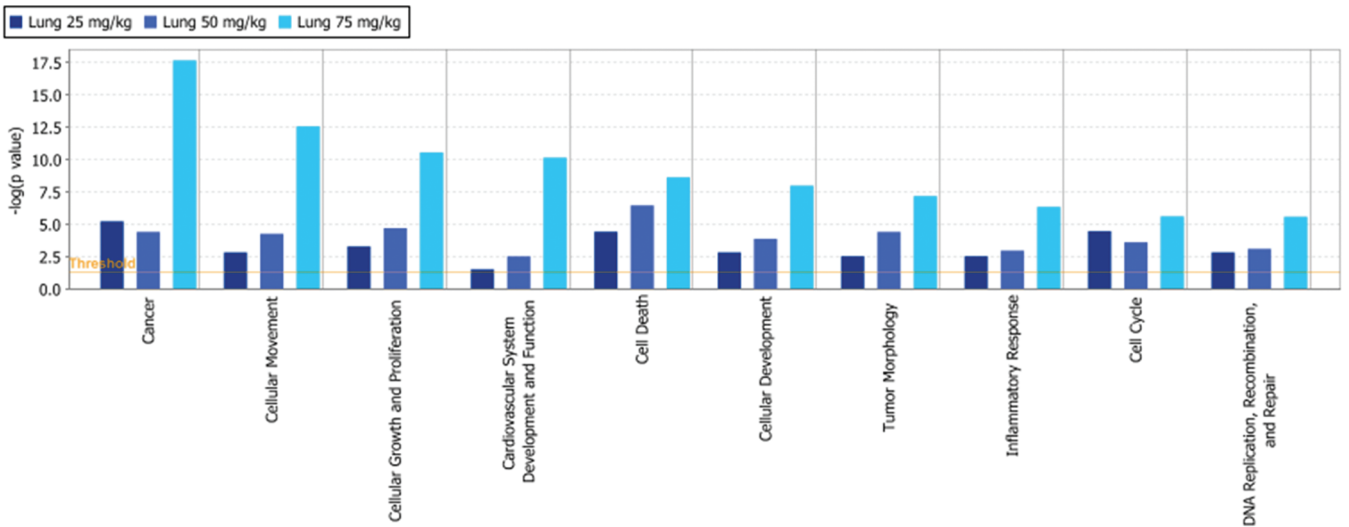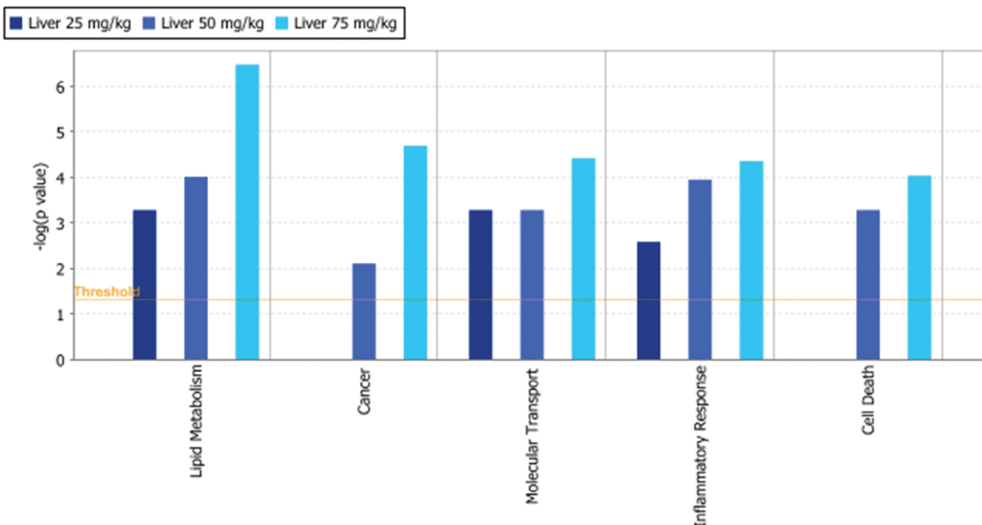
FIG. 2. Functional analysis of differentially expressed genes (FDR adjusted $p \leq 0.1$ and fold change ≥ 1.5 in either direction) using IPA for lung (a) and liver (b). The Ingenuity Pathway Analysis Knowledge Base was used to identify biological functions and/or diseases that were significantly over-represented among the differentially expressed genes. Right-tailed Fisher's exact test was used to calculate a p value determining the probability that each biological function and/or disease assigned to that data set was due to chance alone (threshold set at p value < 0.05).

and were implicated in several biological processes regulated by p53, such as cell cycle arrest, apoptosis, inhibition of cellular growth and proliferation, and DNA repair. Many of these genes were common across the dose groups (Tables 1–3) and showed a clear dose-response. The other affected pathways included the molecular mechanisms of cancer, AhR signaling, BCR signaling, and angiogenesis (Table 3). A similar functional analysis using IPA on liver (Malik *et al.*, 2012) revealed that the altered genes were associated with lipid metabolism, cancer, molecular transport, inflammatory response, and cell death (Fig. 2b). Subanalysis of the cancer-associated genes in the liver reveals that in addition to the p53 signaling pathway, this category includes genes involved in

metabolism and inflammation, which are indirectly linked to carcinogenesis.

Visualization of the relationship between these genes in a biological network created in IPA (Fig. 3) revealed that at the low dose the immediate downstream effectors of p53, such as *Cdkn1a*, *Ccng1*, *Bax*, and *Tp53inp1* mainly involved in DNA damage recognition, cell cycle arrest, and apoptosis were upregulated. However, with increasing dose, genes known to be the suppressors of p53 signaling pathway, such as *Mdm2*, were upregulated along with other genes implicated in proliferation and growth, evasion of apoptosis, promotion of angiogenesis, and cell invasion and metastasis pathways, all of which are the hallmarks of cancer.

TABLE 1
Agilent Probes with FDR Adjusted *p* value ≤ 0.05 Common to All Three Dose Groups as Measured by Microarrays on Lung Tissue

Agilent probe	Accession no.	Gene symbol	Function	25 mg/kg/day	50 mg/kg/day	75 mg/kg/day
A_52_P612803	NM_009831	*Ccng1*	Cell cycle	↑ 1.8	↑ 3.3	↑ 4.6
A_51_P363947	NM_007669	*Cdkn1a*	Cell cycle	↑ 2.5	↑ 5.7	↑ 9.3
A_51_P472751	NM_007915	*Ei24*	Apoptosis	↑ 1.4	↑ 1.8	↑ 2.1
A_51_P508289	NM_010145	*Ephx1*	Xenobiotic metabolism	↑ 1.7	↑ 2.3	↑ 2.9
A_52_P532982	NM_011819	*Gdf15*	Cellular differentiation and proliferation	↑ 2.6	↑ 6.9	↑ 9.1
A_51_P468173	NM_008251	*Hmgn1*	DNA damage repair	↑ 1.3	↑ 1.5	↑ 1.5
A_51_P167489	XM_140451	*Lama3*	Cell adhesion	↑ 1.6	↑ 1.5	↑ 1.5
A_51_P484111	NM_016762	*Matn2*	Unknown function	↓ 1.5	↓ 1.5	↓ 1.9
A_51_P463562	NM_008620	*Mpa2*	Possibly cellular differentiation	↑ 1.4	↑ 1.5	↑ 1.8
A_52_P13389	NM_026793	*Myct1*	Possibly apoptosis	↑ 1.6	↑ 1.8	↑ 1.9
A_51_P195875	NM_010929	*Notch4*	Cellular differentiation	↑ 1.6	↑ 1.7	↑ 1.8
A_51_P363801	NM_023217	*Pgpep1*	Proteolysis	↑ 1.3	↑ 1.6	↑ 1.5
A_51_P329928	NM_013750	*Phlda3*	Apoptosis	↑ 2.1	↑ 3.8	↑ 5.1
A_51_P224564	NM_176833	*Ppm1f*	Apoptosis	↑ 1.4	↑ 1.5	↑ 2.0
A_51_P227392	NM_133955	*Rhou*	Cell cycle	↓ 1.6	↓ 1.6	↓ 1.5
A_51_P246903	NM_026467	*Rps27l*	Apoptosis/DNA damage repair	↑ 1.4	↑ 1.8	↑ 2.5
A_51_P319572	NM_001037709	*Rusc2*	Unknown function	↑ 1.3	↑ 1.5	↑ 1.7
A_51_P415755	AK052232	*Sema6d*	Cellular differentiation	↑ 1.4	↑ 1.4	↑ 1.5
A_52_P154710	AK170547	*Sesn2*	DNA damage repair	↑ 1.7	↑ 2.7	↑ 3.8
A_52_P220810	NM_144551	*Trib2*	Cellular proliferation	↑ 1.4	↑ 1.9	↑ 2.1
A_51_P175580	NM_021897	*Trp53inp1*	Apoptosis	↑ 1.6	↑ 2.5	↑ 2.9
A_52_P503387	NM_021897	*Trp53inp1*	Apoptosis	↑ 1.6	↑ 2.3	↑ 2.9
A_51_P509609	NM_053082	*Tspan4*	Cell signaling	↑ 1.7	↑ 1.7	↑ 1.8
A_51_P155052	NM_053247	*Xlkd1*	Metastasis	↑ 2.2	↑ 2.3	↑ 3.2
A_52_P686785	NM_053247	*Xlkd1*	Metastasis	↑ 2.1	↑ 2.1	↑ 3.6

Note. ↑ indicates upregulated; ↓ indicates downregulated. Fold changes relative to control are shown. The most commonly associated gene function is provided.

RT-PCR Validation of Microarray Results

Exposure to BaP resulted in altered expression of a number of genes involved in the molecular mechanisms of cancer (Table 3). Perturbation of this pathway was confirmed using a cancer pathway-specific PCR array (Mouse Cancer PathwayFinder PCR array, SABiosciences) containing 84 genes. In addition, 61 more genes implicated in BCR signaling, calcium signaling, transforming growth factor beta (TGFβ) signaling, cell cycle, and DNA damage repair pathways were also analyzed (Table 3). From each dose group, five individual samples were analyzed.

In total, 57 of the 145 genes were differentially expressed with $p \leq 0.1$ in at least one treatment group compared with controls (Table 3, Supplementary File 5); 23 of these correlated with the microarray results. Thirty-one genes were significantly differentially expressed as measured by the PCR arrays but not by microarrays. This is presumably due to the enhanced dynamic range and sensitivity of RT-PCR. These genes included baculoviral IAP repeat-containing 5 (*Birc5*), tumor necrosis factor receptor superfamily member 1A (*Tnfrsf1a*), jun proto-oncogene (*Jun*), c-fos-induced growth factor (*Figf*), insulin-like growth factor 1 (*Igf1*), interferon beta 1 fibroblast (*Ifnb1*), vascular endothelial growth factors a and c (*Vegfa* and *Vegfc*), plasminogen activator urokinase (*Plau*), integrin alpha 3 (*Itga3*), platelet-derived growth factors a and b (*Pdgfa* and *Pdgfb*), and transforming growth factor beta 1 (*Tgfb1*) (Table 3).

DISCUSSION

BaP is the only PAH classified by IARC as a known human carcinogen (Baan *et al.*, 2009). The ability to induce DNA damage and mutations in key genes involved in tumor suppression or tumor promotion is one of the postulated mechanisms of BaP-induced carcinogenesis (Denissenko *et al.*, 1996; Ross and Nesnow, 1999). The metabolic activation of BaP by phase I CYP enzymes is a prerequisite for its potentially carcinogenic interaction with DNA (Arlt *et al.*, 2008; Rubin, 2001). Several clinical and epidemiological studies have shown a link between the levels of DNA adducts and exposure-induced carcinogenesis (Gunter *et al.*, 2007; Tang *et al.*, 2001). Thus, the presence of DNA adducts may be a risk factor for developing cancer. Although many tissues are capable of metabolizing BaP to its carcinogenic intermediate, which is associated with the development of mutations, carcinogenesis is specific to certain tissues. For example, BaP is predominantly metabolized in the liver; however, hepatocarcinogenesis is relative-

TABLE 2
p53 Regulated Genes That Were Significantly Differentially Expressed With Microarrays and Real-Time PCR in Lungs

Gene symbol	25 mg/kg/day		50 mg/kg/day		75 mg/kg/day	
	Microarray	RT-PCR	Microarray	RT-PCR	Microarray	RT-PCR
Cdkn1a	↑ 2.5	↑ 3.2	↑ 5.7	↑ 8.1	↑ 9.3	↑ 12.6
Ccng1	↑ 1.7	↑ 2.2	↑ 3.1	↑ 3.0	↑ 4.6	↑ 4.3
Trp53inp1	↑ 1.6	↑ 1.8	↑ 2.4	↑ 2.1	↑ 2.9	↑ 3.2
Sesn2	—	↑ 2.9	↑ 2.2	—	↑ 2.7	↑ 3.4
Bax	↑ 1.5	↑ 1.9	↑ 1.9	↑ 2.5	↑ 2.5	↑ 3.4
Pmaip1	—	—	↑ 1.7	↑ 1.7	↑ 1.7	↑ 1.8
Mdm2	—	—	—	↑ 1.8	↑ 1.6	↑ 2.7
Bcl2	—	—	—	—	—	↑ 1.5
Ccnb2	—	—	—	↑ 1.7	—	↑ 1.9
Tnfrsf10b	—	↑ 2.0	—	↑ 2.7	—	↑ 4.4
Zmat3	—	↑ 1.8	↑ 1.8	↑ 1.7	↑ 2.7	↑ 2.5

Note. ↑ indicates upregulated; — indicates no change. Only genes with FDR adjusted $p \leq 0.1$ and fold change ≥ 1.5 are shown. Gene symbols in bold were also differentially expressed in liver (Malik *et al.*, 2012).

ly less frequent in some experimental animal models and in humans compared with pulmonary carcinogenesis (Hakura *et al.*, 1998; Stoner *et al.*, 1984; Wattenberg and Leong, 1970). Several factors are suggested to play a vital role in the tissue-specific transformation process, including a balance between the metabolic activation and detoxification processes and the relative rates of DNA damage, DNA repair, and individual susceptibility.

The presence of tissue DNA adducts and genetic mutations in genes is often used as a measure of the carcinogenic potential of a chemical (Mei *et al.*, 2006; Wang *et al.*, 2011). Although these markers of exposure and effect, respectively, classify a chemical as genotoxic and nongenotoxic, they may not accurately predict with certainty their carcinogenic potential. We have recently shown that acute exposure to BaP by oral gavage leads to similar levels of DNA adducts in the lungs and livers, two BaP bioactivating organs (Halappanavar *et al.*, 2011). However, despite similar levels of DNA damage (reflective of bioavailable BaP) in both the tissues, the transcriptomic responses in lungs were different and included lung-specific perturbations of several biological pathways associated with

TABLE 3
Genes Validated Using Real-Time PCR Arrays Divided Based on Functional Association in Lungs

Function	Gene symbol	25 mg/kg/day		50 mg/kg/day		75 mg/kg/day	
		Microarray	RT-PCR	Microarray	RT-PCR	Microarray	RT-PCR
p53 signaling	*Cdkn1a*	↑ 2.5	↑ 3.2	↑ 5.7	↑ 8.1	↑ 9.3	↑ 12.6
	*Tnfrsf10b**	—	↑ 2.0	—	↑ 2.7	—	↑ 4.4
	Ccng1	↑ 1.7	↑ 2.2	↑ 3.1	↑ 3.0	↑ 4.6	↑ 4.3
	Bax	↑ 1.5	↑ 1.9	↑ 1.9	↑ 2.5	↑ 2.5	↑ 3.4
	Sesn2	—	↑ 2.9	↑ 2.2	—	↑ 2.7	↑ 3.4
	Trp53inp1	↑ 1.6	↑ 1.8	↑ 2.4	↑ 2.1	↑ 2.9	↑ 3.2
	Mdm2	—	—	—	↑ 1.8	↑ 1.6	↑ 2.7
	Zmat3	—	↑ 1.8	↑ 1.8	↑ 1.7	↑ 2.7	↑ 2.5
	*Ccnb2**	—	—	—	↑ 1.7	—	↑ 1.9
	Pmaip1	—	—	↑ 1.7	↑ 1.7	↑ 1.7	↑ 1.8
	*Bcl2**	—	—	—	—	—	↑ 1.5
B-cell receptor signaling	*Cd3g**	—	—	—	—	—	↓ 1.7
	*Cxcr5**	—	—	—	—	—	↓ 1.5
	*Dock2**	—	—	—	—	—	↓ 1.5
	Tnfsf10	—	↑ 1.5	↑ 1.8	—	↑ 1.8	↑ 1.5
Calcium signaling	*Penk**	—	↑ 2.5	—	—	↓ 2.4	↑ 2.4
	Cyr61	—	↑ 1.5	—	↑ 1.8	↑ 1.9	↑ 1.8
	Adrb1	—	↑ 1.7	—	—	↑ 1.9	↑ 1.7
	Slc30a1	—	—	↑ 1.5	—	↑ 1.5	↑ 1.7
	*S100a8**	—	↓ 1.6	—	—	—	—
	*Pln**	—	↓ 2.4	—	—	—	—
	*Per1**	—	↑ 2.4	—	—	—	—
Transforming growth factor signaling	*Ccnb2*	—	—	—	↑ 1.7	—	↑ 1.9
	Ctgf	—	↑ 1.7	—	↑ 1.6	↑ 1.8	↑ 1.9
	Cyr61	—	↑ 1.5	—	↑ 1.8	↑ 1.9	↑ 1.8
	*Eng**	—	↑ 1.8	—	↑ 1.5	—	↑ 1.6
	*Jun**	—	↑ 1.5	—	—	—	↑ 1.6
	*Igf1**	—	—	—	—	—	↑ 1.5
	*Tgfb1**	—	—	—	—	—	↑ 1.5

TABLE 3—*Continued*

| Function	Gene symbol	25 mg/kg/day		50 mg/kg/day		75 mg/kg/day	
		Microarray	RT-PCR	Microarray	RT-PCI	Microarray	RT-PCR
Cell cycle and DNA damage repair	Cdkn1a	↑ 2.5	↑ 3.2	↑ 5.7	↑ 8.1	↑ 9.3	↑ 12.6
	Sesn2	—	↑ 2.9	↑ 2.2	—	↑ 2.7	↑ 3.4
	Mdm2	—	—	—	↑ 1.8	↑ 1.6	↑ 2.7
	Mgmt*	—	—	—	↑ 2.0	—	↑ 2.7
	Ccnd1	—	—	↑ 1.7	↑ 1.8	↑ 2.3	↑ 2.5
	Polk	—	—	↑ 1.6	↑ 1.6	↑ 1.9	↑ 1.8
	Tgfb1	—	—	—	—	—	↑ 1.5
	Prc1*	—	↑ 1.5	—	—	—	—
Apoptosis	Tnfrsf10b*	—	↑ 2.0	—	↑ 2.7	—	↑ 4.4
	Bax	↑ 1.5	↑ 1.9	↑ 1.9	↑ 2.5	↑ 2.5	↑ 3.4
	Trp53inp1	↑ 1.6	↑ 1.8	↑ 2.4	↑ 2.1	↑ 2.9	↑ 3.2
	Bcl2l1	—	—	—	↑ 1.7	↑ 1.6	↑ 2.3
	Tnfrsf1a*	—	—	—	—	—	↑ 1.7
	Bcl2*	—	—	—	—	—	↑ 1.5
	Tgfb1*	—	—	—	—	—	↑ 1.5
	Tnfsf10	↑ 1.5	↑ 1.5	↑ 1.8	—	↑ 1.8	↑ 1.5
	Cidea*	—	↑ 2.7	—	—	—	—
	Card6*	—	↑ 1.5	—	—	—	—
Angiogenesis	Col18a1	—	—	—	↑ 1.5	↑ 1.8	↑ 2.1
	Cyr61	—	↑ 1.5	—	↑ 1.8	↑ 1.9	↑ 1.8
	Kdr*	—	—	—	—	—	↑ 1.8
	Pdgfa*	—	↑ 1.7	—	↑ 1.5	—	↑ 1.8
	Vegfc*	—	↑ 1.6	—	—	—	↑ 1.7
	Pecam1*	—	—	—	—	—	↑ 1.7
	Igf1	—	—	—	—	—	↑ 1.5
	Pdgfb	—	↑ 1.5	—	—	↑ 1.6	↑ 1.5
	Tgfb1*	—	—	—	—	—	↑ 1.5
	Vegfa*	—	↑ 1.5	—	—	—	—
	F2*	—	↑ 2.9	—	—	—	—
	Plg*	—	↑ 1.9	—	—	—	↑ 1.8
Invasion and metastasis	Serpine1	—	↑ 1.8	↑ 2.0	↑ 3.3	↑ 2.8	↑ 5.0
	Plau*	—	↑ 2.8	—	↑ 2.9	—	↑ 3.1
	Mmp2	—	—	—	—	↑ 1.5	↑ 1.9
	Twist1*	—	↓ 2.9	—	—	—	—
Adhesion	Pecam1	—	—	—	—	—	↑ 1.7
	Itga3*	—	—	—	—	—	↑ 1.5
Signal transduction	Jun	—	↑ 1.5	—	—	—	↑ 1.6
	Myc	—	—	—	↓ *1.5*	—	—

Note. ↑ indicates upregulated; ↓ indicates downregulated; — indicates no change. Only genes with FDR adjusted $p \le 0.1$ and fold change ≥ 1.5 are shown. Genes with an asterisk (*) indicate genes significantly differentially expressed by the PCR array but not significant by microarray. Please note that some genes appear more than once because they are implicated in several functions.

molecular mechanisms of cancer (Halappanavar *et al.*, 2011). The present study was undertaken to further explore the molecular mechanisms underlying such distinct tissue-specific responses and their implication in cancer formation employing a subchronic exposure model.

In agreement with the published literature (Baird *et al.*, 2005), we found that daily exposure to BaP for 28 days resulted in significant genotoxicity as measured by a dose-dependent increase in DNA adduct formation and *lac*Z transgene mutant frequency in the lungs of exposed animals (Fig. 1). Compared with the livers from the same mice, there was a statistically significant 1.8- to 3.3-fold increase (Bonferroni-corrected p value ≤ 0.05) in DNA adduct formation in the lung tissues. In alignment with these results, mRNA expression of DNA polymerase Kappa (*PolK*), necessary for the error-free bypass of

the (+)-trans-BPDE-N^2-dG DNA adduct (Ogi *et al.*, 2002), was significantly upregulated in the lungs (Table 3) but not the liver. In contrast, levels of DNA adducts in liver and lung were comparable in C57BL/6 mice acutely exposed to very high doses of BaP (Halappanavar *et al.*, 2011) (i.e., 150 and 300 mg/kg BaP per day for 3 days, sampled 4 and 24 h after the last exposure). The discrepancy in DNA adduct levels between the acute and subchronic repeated dose study could be simply be due to the amount of total BaP gavaged over time. Compared with the hepatic tissue, rate of clearance of BaP from the lungs occurs slowly resulting in longer retention of BaP in lungs (Harrigan *et al.*, 2004), suggesting that the repeated exposure to BaP over 28 consecutive days may have led to accumulation of BaP in lungs resulting in higher DNA adduct levels. Studies have shown accumulation of DNA adducts in some organs that
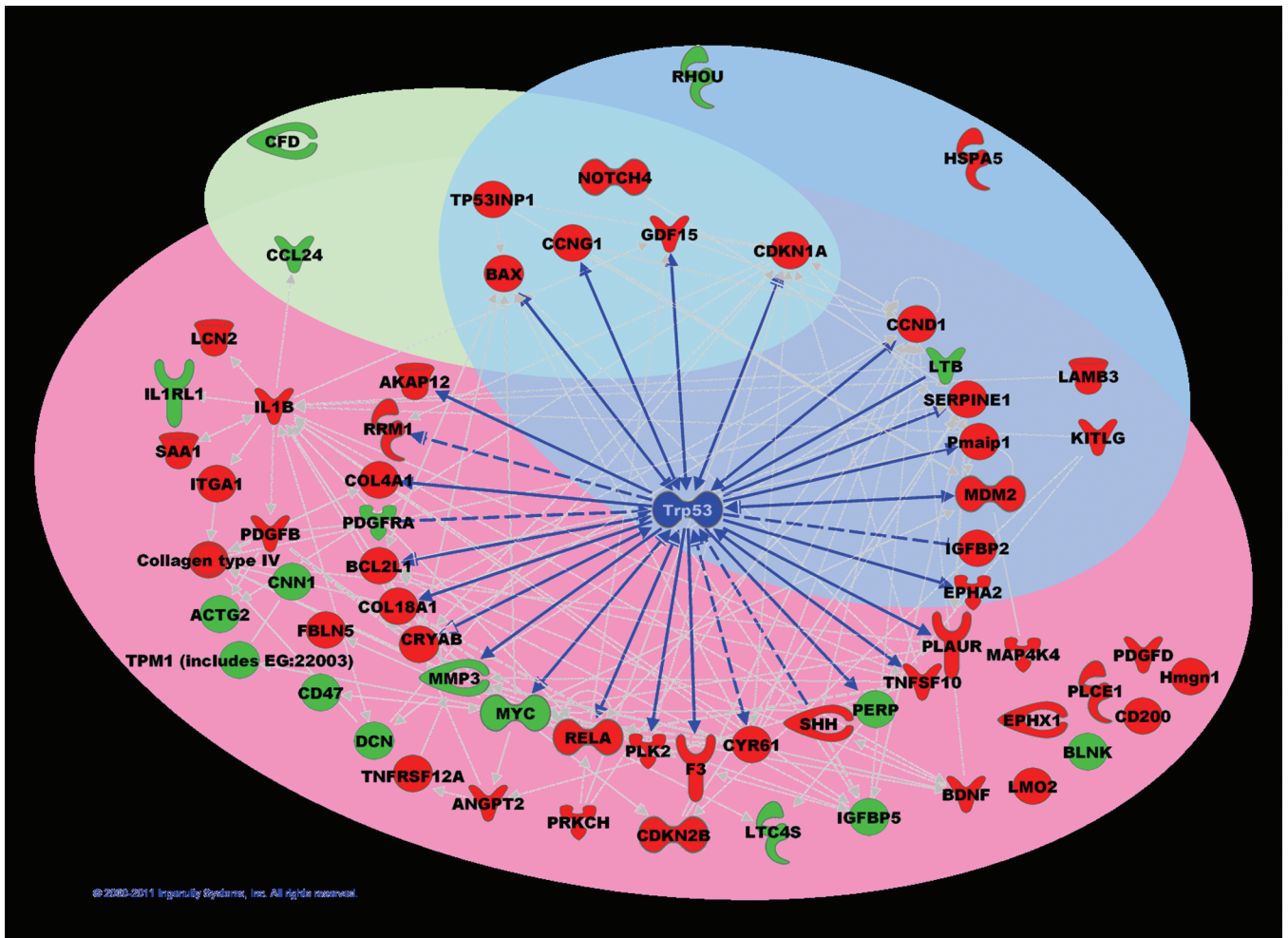
FIG. 3. Molecular relational network of genes modulated by BaP in lung tissues enriched for cancer function using IPA for all three doses with p53 at the central node. A network is a graphical representation of the molecular relationships between molecules. Molecules are represented as nodes and the biological relationship between two nodes is represented as a line. The gene list was derived from cancer-associated genes determined in the Ingenuity Pathway Analysis functional analysis of significantly differentially expressed genes (Fig. 2). The networks were generated from cancer-associated genes differentially regulated in the 25 mg/kg/day (green circle), 50 mg/kg/day (blue circle), and 75 mg/kg/day (pink circle) dose groups. Red color denotes upregulation and green color denotes downregulation.

are resistant to repair or following chronic repeated exposures. It has also been suggested that at higher doses metabolic activation/detoxification of BaP could reach a threshold, which in turn may limit the speed with which reactive metabolites are detoxified in the organ compared with the speed of the translocation of these metabolites from the primary site (e.g., liver) to other distant organs (e.g., lungs).

Although we report significant differences in DNA adduct formation between the lung and liver, the transgene mutant frequency in both tissues was not significantly different, which may suggest more efficient DNA repair in the lungs compared with livers (Fig. 2, high dose). The elevated mutant frequency observed in livers could be attributed to the higher rates of cellular metabolism (as reflected by the number of differentially altered genes in metabolic pathways) potentially resulting in an increase in by-products of reactive oxygen species. These

results suggest that in addition to mutations arising as a result of unrepaired bulky DNA adducts, other factors such as alterations in critical molecular processes implicated in cancer formation may play a role in the selective targeting of the lung tissue for carcinogenesis following BaP exposure.

Our previous work (Halappanavar *et al.*, 2011) on mice acutely exposed to BaP revealed suppression of BCR signaling pathway and an elaborated DNA damage response in the lungs, whereas the livers from the same mice showed subtle changes in only a few genes associated with DNA damage response (Halappanavar *et al.*, 2011). Repressed BCR signaling, leading to primary immunodeficiency, is potentially implicated in cancer initiation (Jumaa *et al.*, 2005). In the present study, we observed similar suppression of a few of the key genes in the BCR signaling pathway in the lungs. However, the response was only observed in the high dose group (Table 2), suggesting

that the collective downregulation of the BCR signaling pathway may be a potential mechanism that operates in the lungs following exposure to high doses of BaP over a very short period of time.

Exposure to BaP for 28 consecutive days induced a large transcriptomic response in the lungs sampled 3 days postexposure compared with the livers. MAANOVA analysis of liver tissue revealed differential expression of 6, 7, and 121 unique probes compared with 20, 145, and 373 probes in the lungs in the 25, 50, and 75 mg/kg exposure groups, respectively (Malik *et al.*, 2012). The p53 signaling pathway was commonly affected in both tissues (Tables 2 and 5) (Malik *et al.*, 2012). p53 is a tumor suppressor protein, and mutations in the *TP53* gene have been found in many types of human cancers linked to environmental exposures (Kucab *et al.*, 2010) including lung cancers. The p53 protein is a transcription factor that mediates expression of several genes, including *Cdkn1a*, an inhibitor of cyclin-dependent kinases, *Bax*, a proapoptotic gene, *Gadd45*, a DNA damage repair gene, which is also involved in cell cycle arrest, and many inflammatory modulators and growth factors. Transgenic mice devoid of *TP53* gene (p53 knockout) or mice in which p53 activity is chemically inhibited exhibit increased susceptibility to develop spontaneous and chemically induced tumors (Donehower *et al.*, 1992). Cellular DNA damage response to BaP is regulated by p53 (Park *et al.*, 2006). Furthermore, increased rates of lung cancer following exposure to BaP arise in transgenic mice expressing lung-specific dominant-negative mutant *p53* (Tchou-Wong *et al.*, 2002), suggesting an important role for the p53 signaling pathway in the development of BaP-induced lung cancer.

Because the focus of the present study was to understand the molecular perturbations in lungs that are associated with tissue-specific tumor development (i.e., relative to the liver), we compared the expression changes of several genes in KEGG pathways associated with cancer in both tissues. Table 4 shows a list of 41 genes whose expression was significantly differentially expressed (FDR $p \leq 0.05$, fold change ≥ 1.5) in lungs but not in the livers. These genes are known for their function in biological pathways such as apoptosis, cell cycle, cytokine-cytokine receptor interaction, extracellular membrane receptor interactions, focal adhesion, mitogen-activated protein kinase signaling, p53 signaling, peroxisome proliferating agent receptor signaling, TGFβ signaling, and Wnt signaling. In contrast, the liver showed expression changes in fewer genes, and these were mainly the downstream effectors of p53 signaling; *Apaf1*, *Trp63*, *MyoD*, *Egr1*, and *Btg2* involved in induction of apoptosis and negative regulation of cellular proliferation. Distinctly affected in the lungs were Sestrin 2 (*Sesn2*), *Pmaip1*, and *Trp53inp1*, associated with the p53-mediated DNA damage response, *Mdm2*, involved in the negative regulation of p53 signaling, and *Bcl2*, implicated in cell survival.

Carcinogenic transformation in the lung following BaP exposure appears to be a dose-dependent process. Figure 3 is

TABLE 4
Cancer Pathway (KEGG) Associated Genes Significantly Differentially Expressed in Microarrays in the Lung and Not in the Liver

Gene symbol	25 mg/ kg/day	50 mg/ kg/day	75 mg/ kg/day	Gene symbol	25 mg/ kg/day	50 mg/ kg/day	75 mg/ kg/day
Bax	—	↑ 1.9	↑ 2.5	*Map4k4*	—	—	↑ 1.8
Bcl2l1	—	—	↑ 1.6	*Mdm2*	—	↑ 1.7	↑ 2.2
Bdnf	—	—	↑ 1.5	*Myc*	—	—	↓ 1.6
Bmp6	—	—	↑ 1.5	*Nkd1*	—	↑ 1.7	↑ 1.9
Ccl5	—	—	↓ 2.1	*Ntrk2*	—	—	↓ 1.6
Cd47	—	—	↓ 1.5	*Pdgfd*	—	—	↑ 1.5
Col4a1	—	—	↑ 1.7	*Pdgfd*	—	—	↑ 1.5
Col4a2	—	—	↑ 1.7	*Pdgfra*	—	—	↓ 1.5
Cpt1b	—	—	↓ 1.6	*Pmaip1*	—	↑ 1.7	↑ 1.8
Cpt1c	—	—	↑ 1.9	*Ptprm*	—	—	↑ 1.6
Dcn	—	—	↓ 2.4	*Rasgrp3*	—	—	↑ 1.8
Ei24	—	↑ 1.8	↑ 2.1	*relA*	—	—	↑ 1.6
Flnc	—	—	↑ 1.7	*Serpine1*	—	↑ 2.0	↑ 2.8
Gp9	—	↑ 1.8	↑ 1.5	*Sesn2*	↑ 1.7	↑ 2.7	↑ 3.8
Itga1	—	—	↑ 1.5	*Smurf2*	—	↑ 1.6	—
Kitl	—	↑ 1.6	↑ 1.6	*Tnfrsf12a*	—	—	↑ 1.7
Lama3	↑ 1.6	↑ 1.5	↑ 1.5	*Tnfsf10*	—	↑ 1.8	↑ 1.8
Lamb3	↑ 1.5	↑ 1.5	↑ 1.6	*Ubc*	—	—	↑ 1.5
Lamc2	—	—	↑ 1.6	*Wnt10a*	—	↓ 1.6	↓ 1.6
Ltb	—	—	↓ 1.5	*Wnt7a*	—	—	↑ 1.8
Map4k1	—	—	↓ 1.5				

Note. ↑ indicates upregulated; ↓ indicates downregulated; — indicates no change. Only genes with FDR adjusted $p \leq 0.05$ and fold change ≥ 1.5 are shown.

TABLE 5
p53 Regulated Genes Identified in Liver by Malik *et al.* (2012) Were Cross Validated in the Lung Using Real-Time PCR Arrays

Gene symbol	25 mg/kg/day Lung	25 mg/kg/day Liver	50 mg/kg/day Lung	50 mg/kg/day Liver	75 mg/kg/day Lung	75 mg/kg/day Liver
Cdkn1a	↑ 3.2	—	↑ 8.1	↑ 6.8	↑ 12.6	↑ 16.9
Tnfrsf10b	↑ 2.0	—	↑ 2.7	↑ 3.7	↑ 4.4	↑ 7.8
Egr	—	—	—	↑ 4.1	—	↑ 6.4
Btg2	—	—	—	↑ 2.2	—	↑ 3.4
Ccnb2	—	—	↑ 1.7	—	↑ 1.9	↑ 2.4
Zmat3	↑ 1.8	—	↑ 1.7	↑ 1.6	↑ 2.5	↑ 2.4
Apaf1	—	—	—	↑ 1.8	—	↑ 2.2
Prc1	—	—	—	—	—	↑ 1.9
Ccng1	↑ 2.2	—	↑ 3.0	—	↑ 4.3	↑ 1.8
Birc5	—	—	—	—	—	↑ 1.8
Myod	—	↓ 2.1	—	↓ 1.6	—	↓ 1.6
Bax	↑ 1.9	—	↑ 2.5	—	↑ 3.4	↑ 1.7
Trp63	—	↓ 2.1	—	↓ 2.5	—	—

Note. ↑ indicates upregulated; ↓ indicates downregulated; — indicates no change. Only genes with FDR adjusted $p \leq 0.1$ and fold change ≥ 1.5 are shown.

a molecular relational network consisting of differentially altered genes in lung tissues enriched for cancer function (using IPA functional categorization) in response to BaP exposure in our model. Interestingly, nearly all genes in the network

were found directly or indirectly connected to the transcription factor p53, which is the main node in the network. At the lowest dose, genes associated with an early response to DNA damage, such as *Cdkn1a* and *Ccng1* involved in cell cycle arrest and *Bax* and *Tp53inp1* involved in the apoptotic process, were upregulated, indicating cellular efforts to halt replication until the damage is repaired. With increasing dose, the p53 DNA damage response pathway continued to be activated. However, activation of pathways and genes implicated in silencing p53 function also became evident. This silencing may be related to AhR-dependent induction of *Mdm2* expression (Pääjärvi *et al.*, 2005), which is a negative regulator of p53 signaling; *Mdm2* was upregulated in the two higher doses. Although an apparent dose-dependent transition in the p53 DNA damage response pathway was observed, at the highest dose, many genes involved in angiogenesis (*Angpt2*, *Bdnf*, *Cyr61*), evasion of apoptosis (*Bcl2l1*, *Cryab*, *Lcn2*, *Rela*), growth signals (*Pdgfb*, *Pdgfd*, *Itga1*, *Notch4*), and invasion and metastasis (*Il1b*, *Mmp3*, *Pdgfra*, *Shh*) were upregulated. These high dose effects are indicative of a shift in the fine cellular dynamics from a protective repair mode to a cellular replication and proliferation mode, which may suggest cellular transformation, potentially a key event in the progression to lung carcinogenesis.

One limitation of the present study is that the responses were investigated in whole tissue. The observed changes reflect the responses of over 40 different cell types. It is clear from the lung DNA adduct and mutant frequency data that the observed changes in molecular pathways are the direct results of BaP metabolism in the lung tissue. However, it should be noted that the influence of circulating factors from other target sites may also contribute to the pulmonary responses.

In conclusion, we show that the BaP-induced DNA adduct levels in lung tissue are comparatively higher than in livers after 28 consecutive days of exposure to increasing doses of BaP by oral gavage. However, the occurrence of fixed mutations was comparable in both tissues suggesting that for certain carcinogens traditional markers of genotoxicity, i.e., tissue DNA adduct levels and mutant frequency may only predict the exposure to the carcinogen and not the carcinogenic outcome. In contrast, dose-dependent transition in p53 DNA-damage response pathway that included tissue protective (adaptive) responses at the lowest dose (e.g., genes involved in cell cycle and apoptosis) to growth and proliferative responses at the highest dose (e.g., growth signals and proproliferation) was distinct to lungs only, suggesting such key biological pathway perturbations occurring early after the exposure may be causal to carcinogenesis in lungs compared with livers.

SUPPLEMENTARY DATA

Supplementary data are available online at http://toxsci.oxfordjournals.org/.

REFERENCES

Arlt, V. M., Stiborová, M., Henderson, C. J., Thiemann, M., Frei, E., Aimová, D., Singh, R., Gamboa da Costa, G., Schmitz, O. J., Farmer, P. B., *et al.* (2008). Metabolic activation of benzo[a]pyrene in vitro by hepatic cytochrome P450 contrasts with detoxification in vivo: Experiments with hepatic cytochrome P450 reductase null mice. *Carcinogenesis* **29,** 656–665.

Baan, R., Grosse, Y., Straif, K., Secretan, B., El Ghissassi, F., Bouvard, V., Benbrahim-Tallaa, L., Guha, N., Freeman, C., Galichet, L., *et al.* (2009). A review of human carcinogens - Part F: Chemical agents and related occupations. *Lancet Oncol.* **10,** 1143–1144.

Baird, W., Hooven, L., and Mahadevan, B. (2005). Carcinogenic polycyclic aromatic hydrocarbon-DNA adducts and mechanism of action. *Environ. Mol. Mutagen.* **45,** 106–114.

Culp, S., Gaylor, D., Sheldon, W., Goldstein, L., and Beland, F. (1998). A comparison of the tumors induced by coal tar and benzo[a]pyrene in a 2-year bioassay. *Carcinogenesis* **19,** 117–124.

Dean, J. H., Luster, M. I., Boorman, G. A., Lauer, L. D., Leubke, R. W., and Lawson, L. (1983). Selective immunosuppression resulting from exposure to the carcinogenic congener of benzopyrene in B6C3F1 mice. *Clin. Exp. Immunol.* **54,** 199–206.

Denissenko, M. F., Pao, A., Tang, M., and Pfeifer, G. P. (1996). Preferential formation of benzo[a]pyrene adducts at lung cancer mutational hotspots in p53. *Science* **274,** 430–432.

Donehower, L., Harvey, M., Slagle, B., McArthur, M., Montgomery, C. J., Butel, J., and Bradley, A. (1992). Mice deficient for p53 are developmentally normal but susceptible to spontaneous tumours. *Nature* **356,** 215–221.

Douglas, G. R., Gingerich, J., Gossen, J. A., and Bartlett, S. (1994). Sequence spectra of spontaneous lacZ gene mutations in transgenic mouse somatic and germline tissues. *Mutagenesis* **9,** 451–458.

Efron, B., and Tibshirani, R. J. (1993). *An Introduction to the Bootstrap*. Chapman & Hall/CRC, Boca Raton, FL.

Galván, N., Teske, D. E., Zhou, G., Moorthy, B., MacWilliams, P. S., Czuprynski, C. J., and Jefcoate, C. R. (2005). Induction of CYP1A1 and CYP1B1 in liver and lung by benzo(a)pyrene and 7,12-d imethylbenz(a)anthracene do not affect distribution of polycyclic hydrocarbons to target tissue: Role of AhR and CYP1B1 in bone marrow cytotoxicity. *Toxicol. Appl. Pharmacol.* **202,** 244–257.

Gunter, M., Divi, R., Kulldorff, M., Vermeulen, R., Haverkos, K., Kuo, M., Strickland, P., Poirier, M., Rothman, N., and Sinha, R. (2007). Leukocyte polycyclic aromatic hydrocarbon-DNA adduct formation and colorectal adenoma. *Carcinogenesis* **28,** 1426–1429.

Hakura, A., Tsutsui, Y., Sonoda, J., Kai, J., Imade, T., Shimada, M., Sugihara, Y., and Mikami, T. (1998). Comparison between in vivo mutagenicity and carcinogenicity in multiple organs by benzo[a]pyrene in the lacZ transgenic mouse (Muta Mouse). *Mut. Res.* **398,** 123–130.

Halappanavar, S., Wu, D., Williams, A., Kuo, B., Godschalk, R. W., van Schooten, F. J., and Yauk, C. L. (2011). Pulmonary gene and microRNA

expression changes in mice exposed to benzo(a)pyrene by oral gavage. *Toxicology* **285,** 133–141.

Harrigan, J. A., McGarrigle, B. P., Sutter, T. R., and Olson, J. R. (2006). Tissue specific induction of cytochrome P450 (CYP) 1A1 and 1B1 in rat liver and lung following in vitro (tissue slice) and in vivo exposure to benzo(a)pyrene. *Toxicol. In Vitro* **20,** 426–438.

Harrigan, J. A., Vezina, C. M., McGarrigle, B. P., Ersing, N., Box, H. C., Maccubbin, A. E., and Olson, J. R. (2004). DNA adduct formation in precision-cut rat liver and lung slices exposed to benzo[a]pyrene. *Toxicol. Sci.* **77,** 307–314.

Hettemer-Frey, H. A., and Travis, C. C. (1991). Benzo(a)pyrene: Environmental partitioning and human exposure. *Toxicol. Ind. Health* **7,** 141–157.

Huang da, W., Sherman, B. T., and Lempicki, R. A. (2009). Systematic and integrative analysis of large gene lists using DAVID bioinformatics resources. *Nat. Protoc.* **4,** 44–57.

Jumaa, H., Hendriks, R. W., and Reth, M. (2005). B cell signaling and tumorigenesis. *Ann. Rev. Immunol.* **23,** 415–445.

Kanehisa, M., and Goto, S. (2000). KEGG: Kyoto encyclopedia of genes and genomes. *Nucleic Acids Res.* **28,** 27–30.

Kerr, M. K., and Churchill, G. A. (2001). Experimental design for gene expression microarrays. *Biostatistics* **2,** 183–201.

Kucab, J., Phillips, D. H., and Arlt, V. M. (2010). Linking environmental carcinogen exposure to TP53 mutations in human tumours using the human TP53 knock-in (Hupki) mouse model. *FEBS J.* **277,** 2567–2583.

Lambert, I. B., Singer, T. M., Boucher, S. E., and Douglas, G. R. (2005). Detailed review of transgenic rodent mutation assays. *Mut. Res.* **590,** 1–280.

Lemieux, C., Douglas, G., Gingerich, J., Phonethepswath, S., Torous, D., Dertinger, S., Phillips, D., Arlt, V., and White, P. (2011). Simultaneous measurement of benzo[a]pyrene-induced Pig-a and lacZ mutations, micronuclei and DNA adducts in Muta™ Mouse. *Environ. Mol. Mutagen.* **52,** 756–765.

Malik, A., Williams, A., Lemieux, C., White, P., and Yauk, C. (2012). Hepatic mRNA, microRNA, and miR-34a-Target responses in mice after 28 days exposure to doses of benzo(a)pyrene that elicit DNA damage and mutation. *Environ. Mol. Mutagen.* **53,** 10–21.

Mei, N., Arlt, V., Phillips, D. H., Heflich, R., and Chen, T. (2006). DNA adduct formation and mutation induction by aristolochic acid in rat kidney and liver. *Mut. Res.* **602,** 83–91.

Office of Environmental Health Hazard Assessment (OEHHA). (2010). Benzo(a)pyrene. In *Public Health Goals for Chemicals in Drinking Water.* http://oehha.ca.gov/water/phg/pdf/091610Benzopyrene.pdf.

Ogi, T., Shinkai, Y., Tanaka, K., and Ohmori, H. (2002). Polkappa protects mammalian cells against the lethal and mutagenic effects of benzo[a]pyrene. *Proc. Natl. Acad. Sci. U.S.A.* **99,** 15548–15553.

Pääjärvi, G., Viluksela, M., Pohjanvirta, R., Stenius, U., and Högberg, J. (2005). TCDD activates Mdm2 and attenuates the p53 response to DNA damaging agents. *Carcinogenesis* **26,** 201–208.

Park, S., Lee, S., Ye, S., Yoon, S., Chung, M., and Choi, J. (2006). Benzo[a]pyrene-induced DNA damage and p53 modulation in human hepatoma HepG2 cells for the identification of potential biomarkers for PAH monitoring and risk assessment. *Toxicol. Lett.* **167,** 27–33.

Phillips, D. H., and Arlt, V. M. (2007). The ^{32}P-postlabeling assay for DNA adducts. *Nat. Protoc.* **2,** 2772–2781.

Qamar, W., Khan, A., Khan, R., Lateef, A., Tahir, M., Rehman, M., Ali, F., and Sultana, S. (2012). Benzo(a)pyrene-induced pulmonary inflammation, edema, surfactant dysfunction, and injuries in rats: Alleviation by farnesol. *Exp. Lung Res.* **38,** 19–27.

R-Development-Core-Team. (2010). *R: A Language and Environment for Statistical Computing.* R Foundation for Statistical Computing, Vienna, Austria.

Renault, D., Brault, D., and Thybaud, V. (1997). Effect of ethylnitrosourea and methyl methanesulfonate on mutation frequency in Muta™Mouse germ cells seminiferous tubule cells and epididymis spermatozoa. *Mut. Res.* **388,** 145–153.

Ross, J. A., and Nesnow, S. (1999). Polycyclic aromatic hydrocarbons: Correlations between DNA adducts and ras oncogene mutations. *Mut. Res.* **424,** 155–166.

Rubin, H. (2001). Differential regulation of similar lung-specific biological processes implicated in cancer formation occur at lower doses and may potentially help predict the long-term impact and health effects of benzo(a) pyrene exposure. *Carcinogenesis* **22,** 1903–1930.

Shwed, P. S., Crosthwait, J., Douglas, G. R., and Seligy, V. L. (2010). Characterisation of MutaMouse lambdagt10-lacZ transgene: Evidence for in vivo rearrangements. *Mutagenesis* **25,** 609–616.

Solhaug, A., Øvrebø, S., Mollerup, S., Låg, M., Schwarze, P., Nesnow, S., and Holme, J. (2005). Role of cell signaling in B[a]P-induced apoptosis: Characterization of unspecific effects of cell signaling inhibitors and apoptotic effects of B[a]P metabolites. *Chem. Biol. Interact.* **151,** 101–119.

Stoner, G. D., Greisiger, E. A., Schut, H. A., Pereira, M. A., Loeb, T. R., Klaunig, J. E., and Branstetter, D. G. (1984). A comparison of the lung adenoma response in strain A/J mice after intraperitoneal and oral administration of carcinogens. *Toxicol. Appl. Pharmacol.* **72,** 313–323.

Tang, D., Phillips, D., Stampfer, M., Mooney, L., Hsu, Y., Cho, S., Tsai, W., Ma, J., Cole, K., Shé, M. *et al.* (2001). Association between carcinogen-DNA adducts in white blood cells and lung cancer risk in the physicians health study. *Cancer Res.* **61,** 6708–6712.

Tchou-Wong, K., Jiang, Y., Yee, H., LaRosa, J., Lee, T., Pellicer, A., Jagirdar, J., Gordon, T., Goldberg, J., and Rom, W. (2002). Lung-specific expression of dominant-negative mutant p53 in transgenic mice increases spontaneous and benzo(a)pyrene-induced lung cancer. *Am. J. Respir. Cell Mol. Biol.* **27,** 186–193.

Vijg, J., and Douglas, G. R. (1996). Bacteriophage lambda and plasmid lacZ transgenic mice for studying mutations in vivo. In *Technologies for Detection of DNA Damage and Mutations* (G. Pfeifer, Ed.), pp. 391–410. Plenum Press, New York, NY.

Wang, Y., Meng, F., Arlt, V. M., Mei, N., and Chen, T. (2011). Aristolochic acid-induced carcinogenesis examined by ACB-PCR quantification of H-Ras and K-Ras mutant fraction. *Mutagenesis* **26,** 619–628.

Wattenberg, L. W., and Leong, J. L. (1970). Inhibition of the carcinogenic action of benzo(a)pyrene by flavones. *Cancer Res.* **30,** 1922–1925.

Wu, H., Yang, H., Sheppard, K., Churchill, G., Kerr, K. and Cui, X. (2010). *MAANOVA: Tools for analyzing microarray experiments.* Version 1.20.0.

Yauk, C. L., Jackson, K., Malowany, M., and Williams, A. (2011). Lack of change in microRNA expression in adult mouse liver following treatment with benzo(a)pyrene despite robust mRNA transcriptional response. *Mut. Res.* **722,** 131–139.